

Halogen Atom Regulation of Acceptor-Donor-Acceptor Type Conjugated Molecules for Photothermal Antibacterial and Antibiofilm Therapy

Yue Zhao^a, Yuanyuan Cui^a, Shijie Xie^b, Ruilian Qi^a, Li Xu^{b*}, Huanxiang Yuan^{a*}

^a Department of Chemistry, College of Chemistry and Materials Engineering, Beijing Technology and Business University, Beijing 100048, China.

^b Department of Pharmacy, Hubei University of Chinese Medicine, Wuhan 430065, China.

Materials and Instruments

All analytical grade solvents and reagents were purchased commercially without any purification or treatment. The UV-V is absorption spectra were determined by JASCO V-550 spectrophotometer. The Nano ZS (ZEN3600) system was used to measure the hydrodynamic diameter of the NPs. Amp^r *E. coli*, *S. aureus*, and MRSA were obtained from the National Center for Conservation and Management of General Microbial Species, China. A Fluke Ti400-EN infrared camera was used to record temperature and collect infrared images.

Preparation of BTP-BrCl/BTP-ClBr/BTP-ClmBr NPs

BTP-BrCl/BTP-ClBr/BTP-ClmBr NPs were prepared by a typical nanocoprecipitation method. 0.3 mL of THF solution of BTP-BrCl/BTP-ClBr/BTP-ClmBr (1 mg/mL, dissolved in THF) was mixed evenly with 0.1875 mL of DSPE-PEG2000 (16 mg/mL, dissolved in THF). The resulting mixture was quickly added to 10 mL of deionized water and sonicated in an ultrasonic bath for 2 h followed by heating to remove THF to yield BTP-BrCl/BTP-ClBr/BTP-ClmBr NPs at a final concentration of 100 µg/mL. Finally, the NPs were further processed by filtration through a 0.45 µm PVDF syringe.

Determination of UV-Vis absorption spectra

The UV-Vis absorption spectra of the NPs solution were tested using a UV-Vis absorption spectrometer. The test wavelength was set between 400 and 1000 nm, and the scanning speed was medium. The NPs solution was diluted to 25 $\mu\text{g/mL}$ and tested in a quartz cuvette.

Characterization of photothermal properties

1. Determination of the photothermal conversion capacity of different materials

The aqueous solution of photothermal materials (25 $\mu\text{g/mL}$) was irradiated by 808 nm near-infrared laser at the intensity of 1 W/cm^2 for 5 min, and the temperature change data was recorded every 30 s. Under the same conditions, ultrapure water was used as the experimental control.

2. Determination of concentration and light intensity dependence

NPs dispersions with different concentrations (12.5, 25, 50, 100 $\mu\text{g/mL}$) were irradiated by 808 nm near infrared laser at the intensity of 1 W/cm^2 for 5 min, and temperature changes were recorded at the interval of 30 s. The photothermal conversion characteristics of NPs (25 $\mu\text{g/mL}$, 100 μL) irradiated with different laser power densities (0.5, 0.75, 1.0, 1.5 W/cm^2) were investigated. Under the same conditions, ultrapure water was used as the experimental control.

3. Cyclic stability experiment

100 μL of NPs water dispersion (10 $\mu\text{g/mL}$) was irradiated under 808 nm near-infrared laser with power density of 1 W/cm^2 for 5 min. Temperature changes were measured at the interval of 30 s. After laser irradiation was turned off, temperature change data were recorded again at the same time interval for 5 min, and the ON/OFF cycle was repeated 5 times.

4. Calculation of photothermal conversion efficiency (η)

The calculation method of the photothermal conversion efficiency of NPs is referred to the literature. η is calculated from Equation (1).

$$\eta = \frac{hA(T_{Max} - T_{Surr}) - Q_{Dis}}{I(1 - 10^{-A_{808}})} \quad (1)$$

Where A represents the surface area using the container, and h represents the heat transfer coefficient. A_{808} is the absorbance value of the nanoparticles at 808 nm, and I is the incident laser power (800 mW/cm²). T_{Max} is the highest steady-state temperature, and T_{Surr} is the ambient temperature of the surrounding environment. τ_S is given by the slope of the negative natural logarithm curve of the temperature change during cooling, and the value of τ_S is derived from Equation (2).

$$t = -\tau_S \ln(\theta) = -\tau_S \ln\left(\frac{T_t - T_{Surr}}{T_{Max} - T_{Surr}}\right) \quad (2)$$

Where t is the cooling time point after continuous irradiation, and T_t is the temperature value at the corresponding time point during the cooling process. hA can be calculated from Equation (3).

$$\tau_S = \frac{m_D c_D}{hA} \quad (3)$$

Where m_D and c_D denote mass and heat capacity, respectively. hA is the heat dissipation of the solvent and quartz sample cell, which can be calculated according to Equation (4).

$$Q_{Dis} = \frac{c_D m_D (T_{Max(water)} - T_{Surr})}{\tau_{S(water)}} \quad (4)$$

$T_{Max(water)}$ is the highest steady-state temperature of ultrapure water.

Antibacterial experiment

1. Microbial culture

A single colony of Amp^r *E. coli* was isolated on LB (Luria-Bertani) solid AGAR plates, and 50 µg/mL ampicillin was added and transferred to LB liquid culture (10 mL). The bacteria were incubated at 37 °C for 6-12 h, centrifuged (7100 rpm, 3 min), and washed twice with phosphate buffer saline (1×PBS, pH=7.4). The resulting Amp^r *E. coli* was resuspended in sterile 1×PBS and diluted to a suspension of optical density 1.0 at 600 nm (OD₆₀₀=1.0). In the same way, MRSA and *S. aureus* were cultured in LB

and NB (Nutrient Broth) medium, respectively, and microbial suspensions with $OD_{600}=1.0$ of MRSA and *S. aureus* were prepared.

2. Evaluation of antibacterial activity of NPs solution

First, 20 μL of Amp^r *E. coli* ($OD_{600}=1.0$) mixed with different concentrations of NPs (0, 5, 7.5, 10 $\mu\text{g}/\text{mL}$) was incubated at 37 °C for 30 min in the dark. These Amp^r *E. coli* suspensions were then placed in the dark or irradiated with an 808 nm laser (550 mW/cm^2) for 5 min. Finally, each group was sequentially diluted 5×10^4 times with PBS solution. Then 100 μL of the dilution was spread onto solid agar plates of LB and incubated at 37 °C for 16 to 18 h to form colonies. *S. aureus*/MRSA was operated in the same way as Amp^r *E. coli*, where NB was selected for solid agar plates of *S. aureus*. Inhibition rate (IR) was determined according to the following formula:

$$\text{IR} = (C - C_0) / C_0 \times 100\%$$

Where C is the colony forming units (CFU) of the experimental group, and C_0 is the number of CFU of the control group.

3. Scanning electron microscopy (SEM) characterization

The mixture of NPs and Amp^r *E. coli* treated with the same procedures as in the antibacterial experiment was centrifuged (10,000 rpm, 10 min), and 100 μL of 2.5% glutaraldehyde was added to the precipitate and fixed at 4 °C overnight. After centrifugation (10,000 rpm, 10 min), the precipitate was added to 10 μL of 1×PBS and mixed. After 5 μL of Amp^r *E. coli* suspension was placed on a clean silicon wafer and washed twice with sterile water, 40%, 70%, 90%, and 100% ethanol were added and eluted for 6 min, respectively. Gradient dehydration was completed and measured after drying. *S. aureus*/MRSA had the same procedure.

Inhibition of biofilm formation assay

A suspension (20 $\mu\text{g}/\text{mL}$) of 100 μL *S. aureus* ($OD_{600}=1.0$) mixed with BTP-ClmBr NPs was first incubated at 37 °C for 30 min in the dark. The *S. aureus* suspension was then exposed to a laser at 808 nm with an intensity of 550 mW/cm^2 for 5 min. After irradiation, the mixture was added to 0.25% TSB medium to obtain a 1:100-fold dilution of the bacterial solution. 100 μL of bacteria solution-TSB medium mixture was

added to each well of a 96-well plate and cultured in an incubator at 37 °C for 12, 18, and 24 hours, respectively. TSB medium was washed off by adding 115 µL PBS to each well, repeated 2-3 times, and left to dry. 100 µL of 0.1% crystal violet staining solution was added to each well and stained for 15 min at room temperature. The dye removal solution was washed more than 3 times with 150 µL sterile water per well and left to dry. 100 µL of 10% glacial acetic acid was added to each well and incubated for 30 min in an incubator at 37 °C. Absorbance at a wavelength of 590 nm was measured using a microplate reader. The same procedure was used for BTP-BrCl NPs and BTP-ClBr NPs.

Biofilm disruption assay

A total of 100 µL *S. aureus* was mixed in 0.25% TSB medium, then added to a 96-well plate, and 100 µL of the solution was mixed in each well. The cells were cultured in an incubator at 37 °C for 24 hours. The medium was removed and 100 µL of 15 µg/mL solution of BTP-ClmBr NPs was added to each well and irradiated with a laser at 808 nm and 1W/cm² for 10 min. The solution of BTP-ClmBr NPs was aspirated and 30 µL of PBS was added to each well and sonicated for 10 min. 70 µL of PBS was added to the mixed solution and mixed. After a 50,000-fold dilution, 100 µL of the dilution was spread onto NB solid agar plates and incubated at 37 °C for 16 to 18 h to form colonies. The same procedure was used for BTP-BrCl NPs and BTP-ClBr NPs. Inhibition rate (IR) was determined according to the following formula:

$$IR=(C-C_0)/C_0\times 100\%$$

Where C is the CFU of the experimental group, and C₀ is the number of CFU of the control group.

Blood compatibility test

1 mL of fresh rabbit blood was centrifuged at 5000 rpm for 10 min to remove the supernatant and intermediate leukocytes. 2% red blood cell solution was prepared by adding 20 µL of blood cell precipitate to 980 µL of normal saline. 20 µL Triton X100 was added to the positive control group, and saline was used as the negative control

solvent. The same proportion of NPs dispersing solution was added to the experimental group. The mixture was allowed to stand for 3 h and then centrifuged at 10,000 rpm for 2 min, and the supernatant was collected in a 96-well plate for detection of the absorption value at 541 nm. The hemolysis rate (%) was calculated as follows:

$$\text{Hemolysis ratio (\%)} = \frac{I - I_0}{I' - I_0} \times 100\%$$

Where I is the absorbance of the sample itself, I_0 is the absorbance of the negative control, and I' is the absorbance of the positive control.

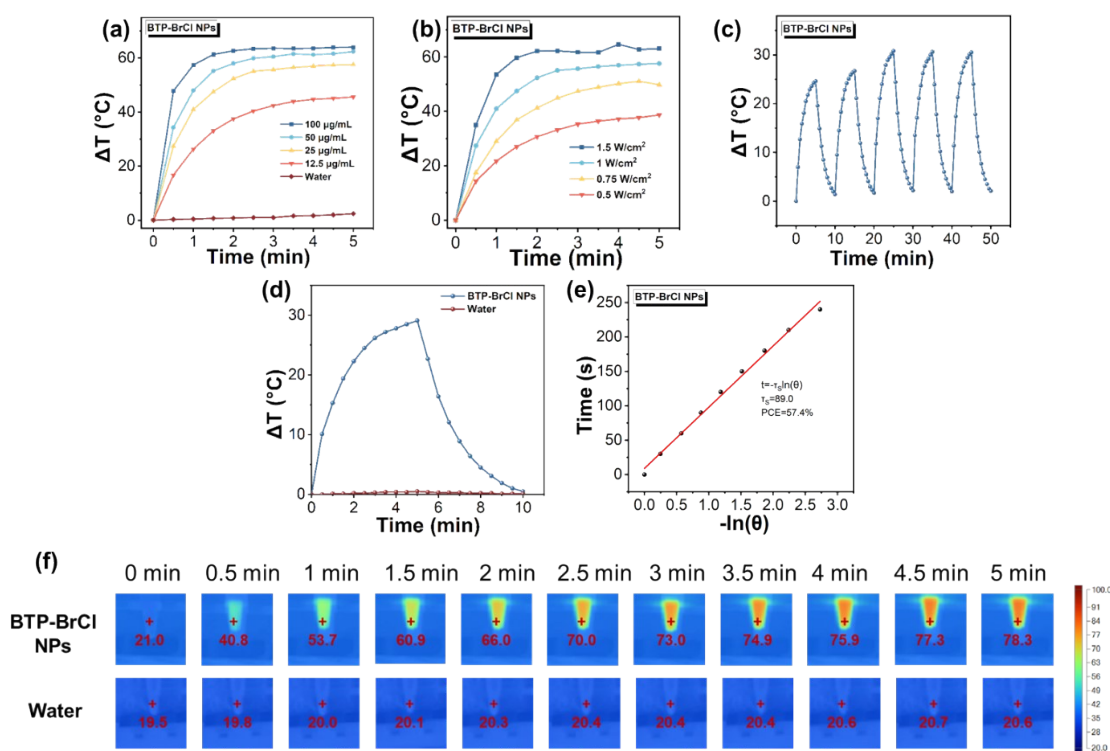


Figure S1. (a) Heating curves of water dispersions of BTP-BrCl NPs irradiated with 808 nm laser (1 W/cm²) at different concentrations. (b) Heating curves of water dispersions of BTP-BrCl NPs (25 µg/mL) at different laser power densities. (c) Heating and cooling cycle curves of five ON/OFF cycles of BTP-BrCl NPs dispersed (10µg/mL) under 808 nm laser irradiation (800 mW/cm²). (d, e) Photothermal properties of BTP-BrCl NPs after cooling to room temperature. (f) Infrared thermogram of BTP-BrCl NPs (10 µg/mL) increasing with irradiation time (808 nm, 800 mW/cm²).

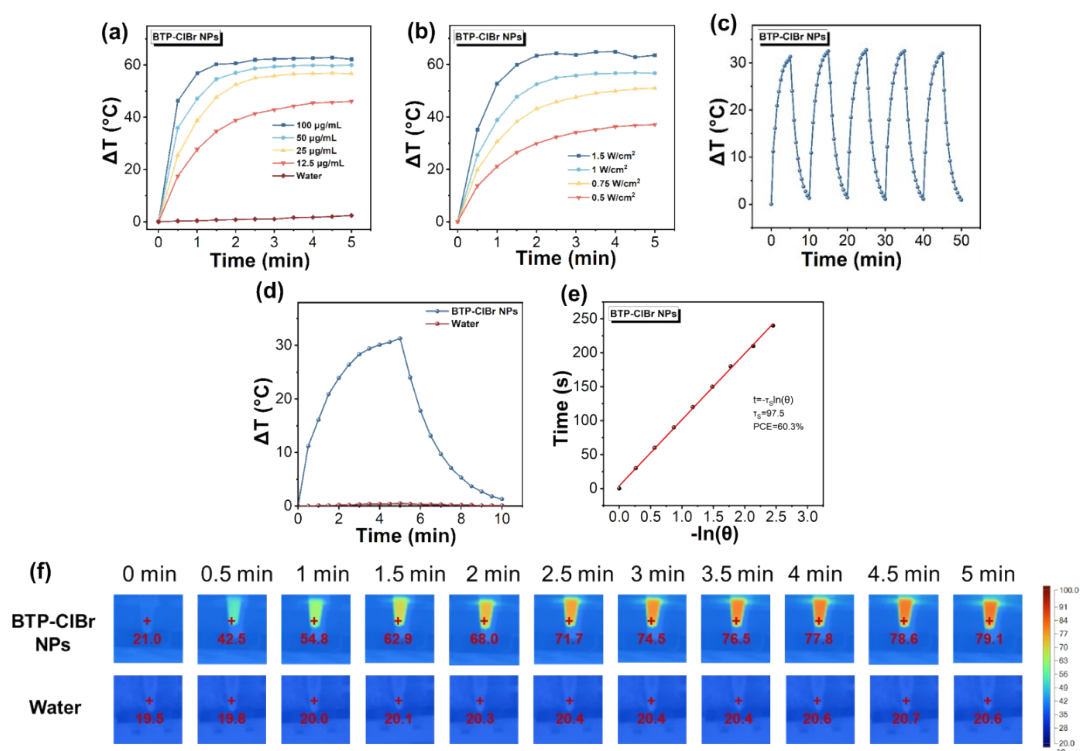


Figure S2. (a) Heating curves of water dispersions of BTP-CIBr NPs irradiated with 808 nm laser (1 W/cm^2) at different concentrations. (b) Heating curves of water dispersions of BTP-CIBr NPs ($25 \mu\text{g/mL}$) at different laser power densities. (c) Heating and cooling cycle curves of five ON/OFF cycles of BTP-CIBr NPs dispersed ($10\mu\text{g/mL}$) under 808 nm laser irradiation (800 mW/cm^2). (d, e) Photothermal properties of BTP-CIBr NPs after cooling to room temperature. (f) Infrared thermogram of BTP-CIBr NPs ($10 \mu\text{g/mL}$) increasing with irradiation time (808 nm, 800 mW/cm^2).

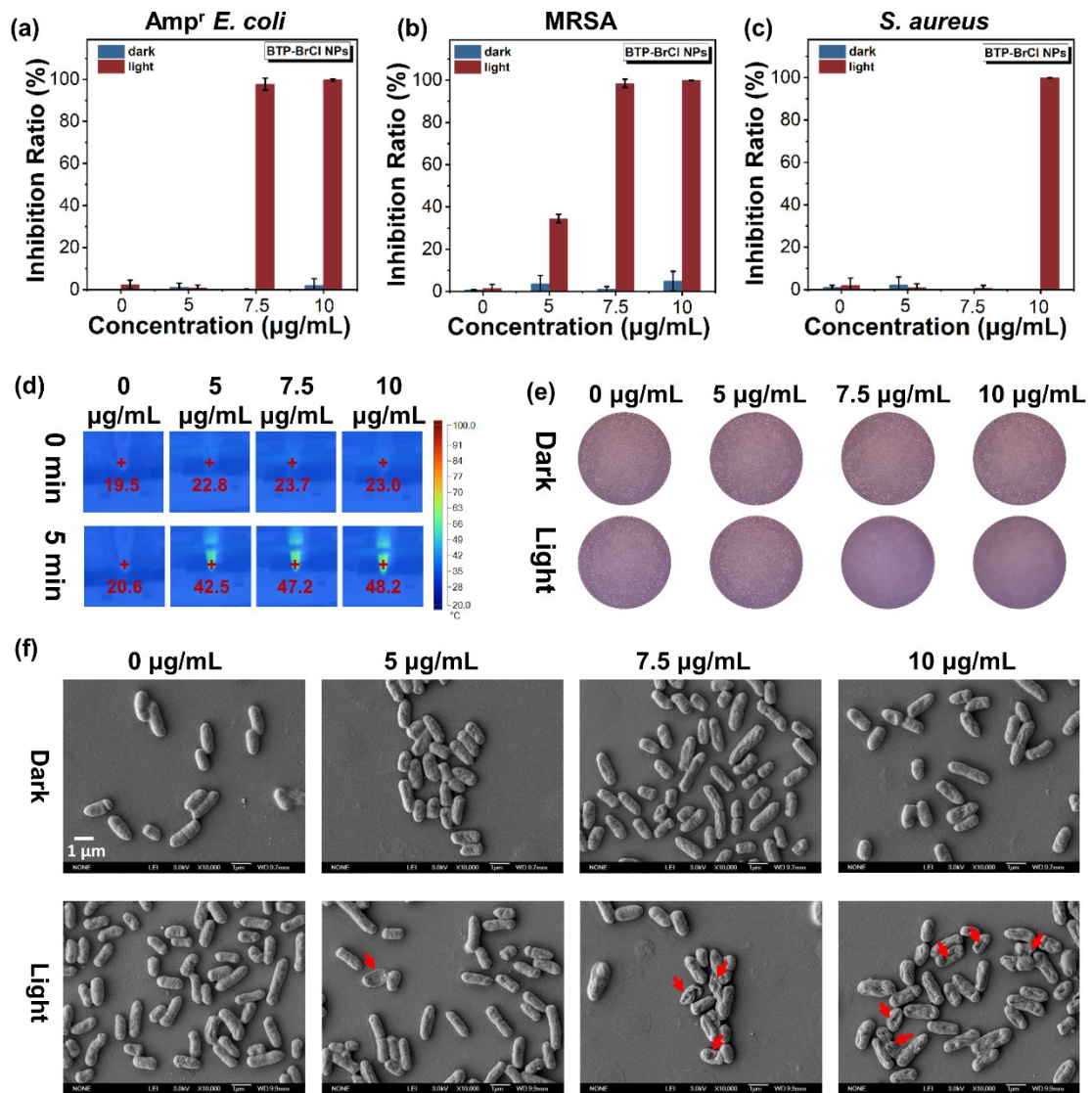


Figure S3. Antibacterial activity of BTP-BrCl NPs against (a) Amp^r *E. coli*, (b) *S. aureus*, and (c) MRSA in the dark or irradiated with 808 nm laser (550 mW/cm²) for 5 min. (d) Corresponding infrared thermography of Amp^r *E. coli* treated with different concentrations of BTP-BrCl NPs at 0 and 5 min of irradiation. (e) Photographs of Amp^r *E. coli* solid plates treated with different concentrations of BTP-BrCl NPs. (f) SEM images of Amp^r *E. coli* treated with different concentrations of BTP-BrCl NPs. Scale bar: 1 μm

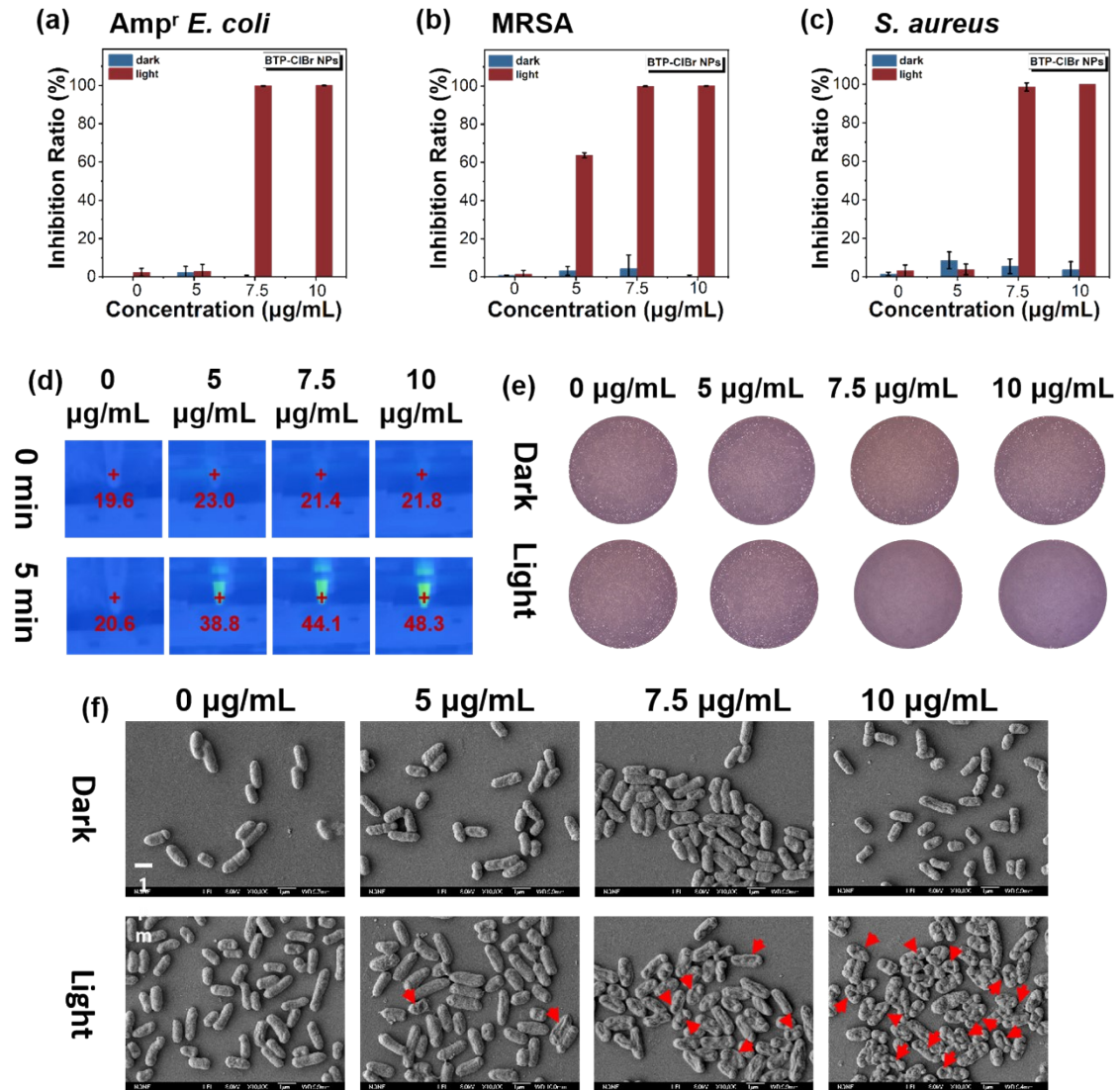


Figure S4. Antibacterial activity of BTP-ClBr NPs against (a) Amp^r *E. coli*, (b) *S. aureus*, and (c) MRSA in the dark or irradiated with 808 nm laser (550 mW/cm²) for 5 min. (d) Corresponding infrared thermography of Amp^r *E. coli* treated with different concentrations of BTP-ClBr NPs at 0 and 5 min of irradiation. (e) Photographs of Amp^r *E. coli* solid plates treated with different concentrations of BTP-BrCl NPs. (f) SEM images of Amp^r *E. coli* treated with different concentrations of BTP-ClBr NPs. Scale bar: 1 μm

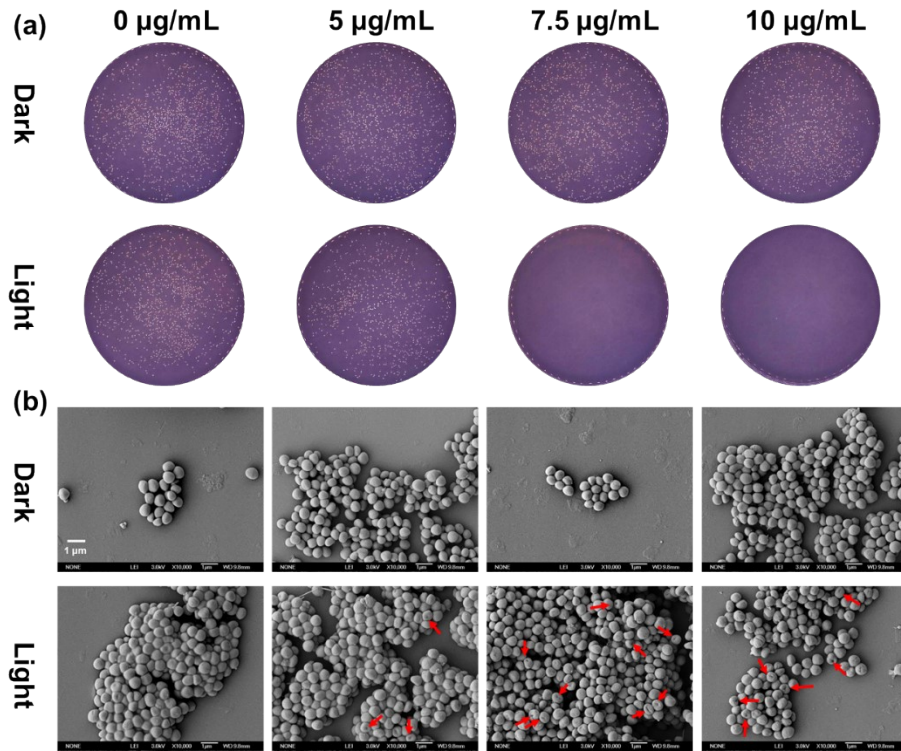


Figure S5. (a) Photos of *S. aureus* solid plates treated with different concentrations of BTP-BrCl NPs. (b) SEM images of *S. aureus* treated with different concentrations of BTP-BrCl NPs. Scale bar: 1 μm

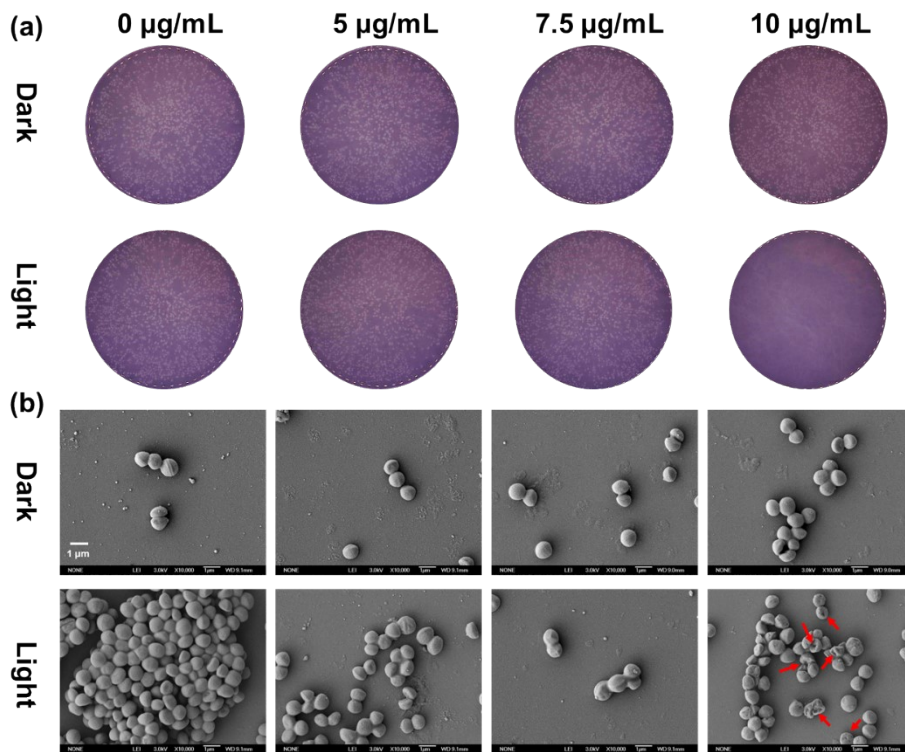


Figure S6. (a) Photos of MRSA solid plates treated with different concentrations of BTP-BrCl NPs. (b) SEM images of MRSA treated with different concentrations of BTP-BrCl NPs. Scale bar: 1 μm

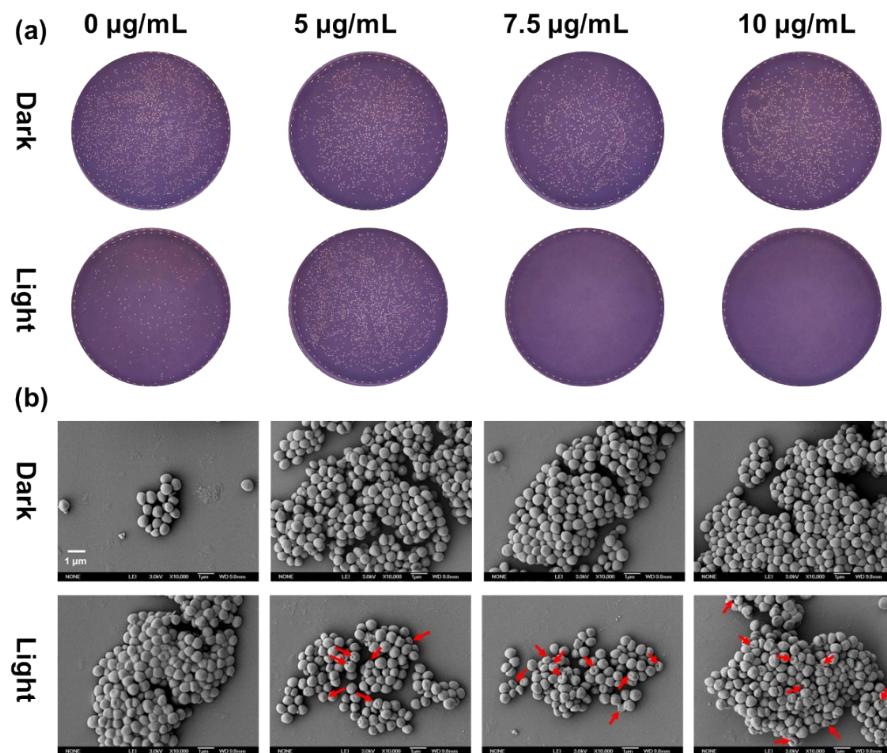


Figure S7. (a) Photos of *S. aureus* solid plates treated with different concentrations of BTP-ClBr NPs. (b) SEM images of *S. aureus* treated with different concentrations of BTP-ClBr NPs. Scale bar: 1 μm

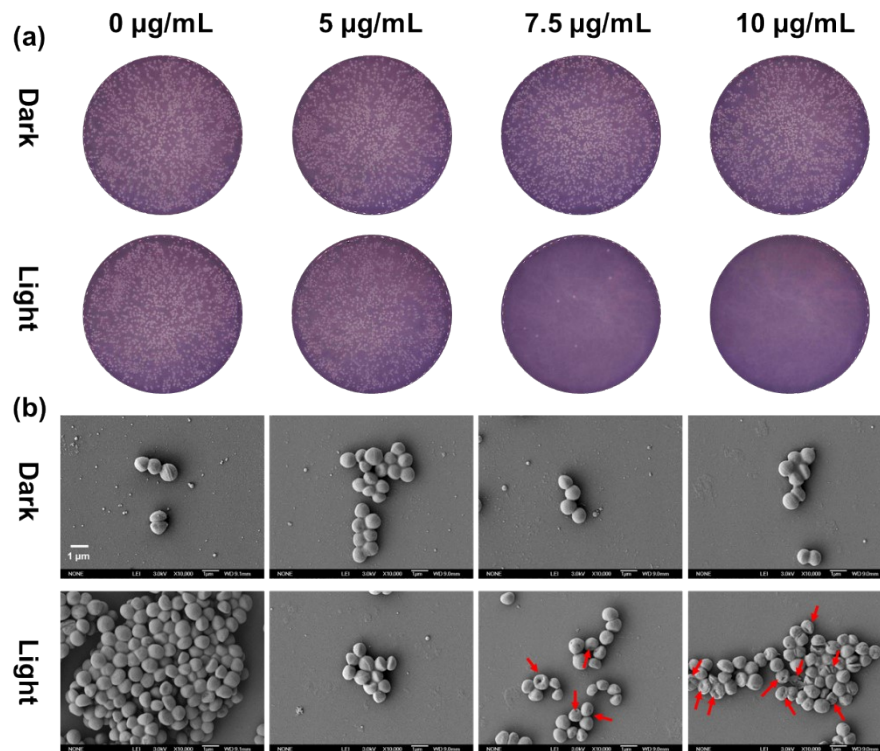


Figure S8. (a) Photos of MRSA solid plates treated with different concentrations of BTP-ClBr NPs. (b) SEM images of MRSA treated with different concentrations of BTP-ClBr NPs. Scale bar: 1 μm

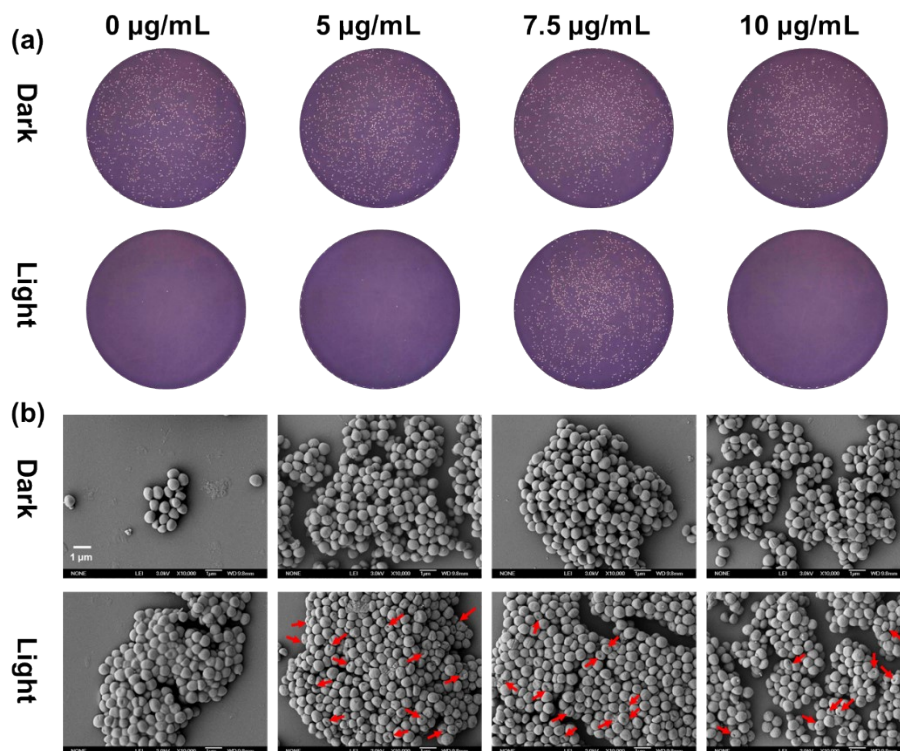


Figure S9. (a) Photos of *S. aureus* solid plates treated with different concentrations of BTP-ClmBr NPs. (b) SEM images of *S. aureus* treated with different concentrations of BTP-ClmBr NPs. Scale bar: 1 μm

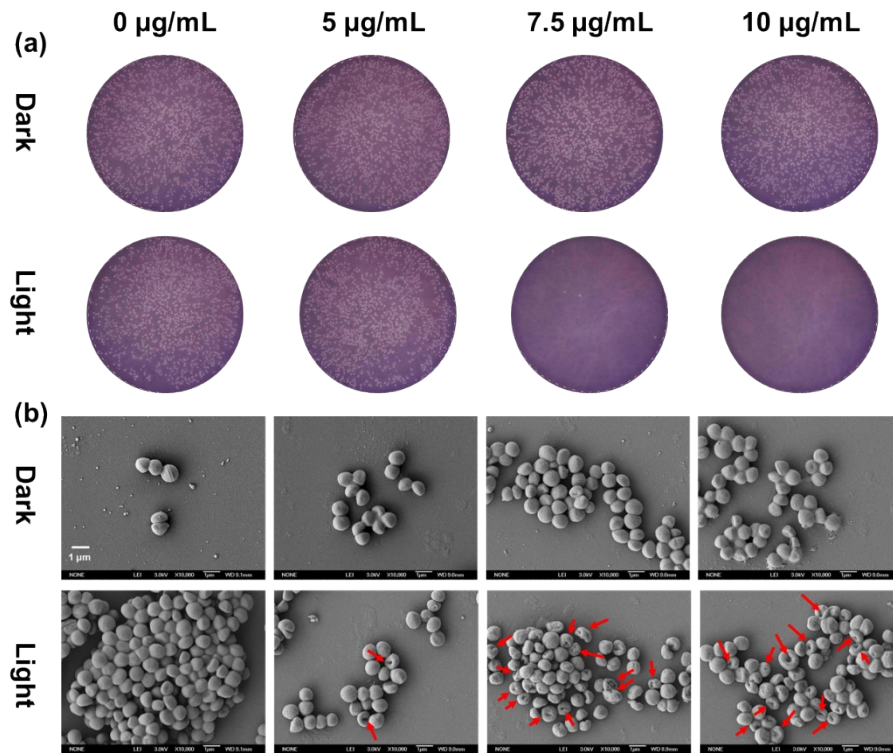


Figure S10. (a) Photos of MRSA solid plates treated with different concentrations of BTP-ClmBr NPs. (b) SEM images of MRSA treated with different concentrations of BTP-ClmBr NPs. Scale bar: 1 μm